

# Substantial organic impurities at the surface of synthetic ammonium sulfate particles

Junteng Wu<sup>1</sup>, Nicolas Brun<sup>1</sup>, Juan Miguel González-Sánchez<sup>1</sup>, Badr R'Mili<sup>1</sup>, Brice Temime Roussel<sup>1</sup>, Sylvain Ravier<sup>1</sup>, Jean-Louis Clément<sup>2</sup>, Anne Monod<sup>1</sup>

5 <sup>1</sup>Aix Marseille Univ, CNRS, LCE, Marseille, France

<sup>2</sup>Aix Marseille Univ, CNRS, ICR, Marseille, France

*Correspondence to:* Junteng Wu (junteng.wu@univ-amu.fr) and Anne Monod (anne.monod@univ-amu.fr)

## Abstract

Ammonium sulfate (AS) particles are widely used for studying the physical-chemistry processes of aerosols and for  
10 instrument calibrations. Small quantities of organic matter can greatly influence the studied properties, as observed by many  
laboratory studies. In this work, monodisperse particles (200 nm to 500 nm aerodynamic diameter) were generated by  
nebulizing various AS solutions and organic impurities were quantified relative to sulfate using a High-Resolution Time-of-  
Flight Aerosol Mass Spectrometer (HR-ToF-AMS). The organic content found in AS solutions was also tentatively identified  
15 using a Liquid Chromatography–tandem Mass Spectrometer (LC-MS). The results from both analytical techniques were  
consistent and demonstrated that the organic impurities contained oxygen, nitrogen and/or sulfur, their molecular masses  
ranged from  $m/z$  69 to 420, they likely originate from the commercial AS crystals. For AS particle sizes ranging from 200 nm  
to 500 nm, the total mass fraction of organic (relative to sulfate) ranged from 3.8 % to 1.5 %, respectively. An inorganic-  
organic mixture model suggested that the organic impurities were coated on the AS particle with a surface density of  $1.1 \times 10^{-3}$   
20  $\text{g}\cdot\text{m}^{-2}$ . A series of tests were performed to remove the organic content (using pure  $\text{N}_2$  in the flow, ultrapure water in the  
solutions, and very high AS quality), showing that at least 40 % of the organic impurities could be removed. In conclusion, it  
is recommended to use AS seeds with caution, especially when small particles are used, in terms of AS purity and water purity  
when aqueous solutions are used for atomization.

## 1 Introduction

Atmospheric aerosols are generally a complex mixture of inorganic and organic compounds that have a strong impact  
25 on climate and human health (IPCC, 2013; Pöschl and Shiraiwa, 2015). According to the annual aerosol emission inventories,  
inorganic compounds account for the majority of the mass (Andreae and Rosenfeld, 2008). Among them, ammonium sulfate  
(AS) is considered as one of the dominant components (Charlson et al., 1992; Seinfeld et al., 2016). Because AS plays  
important roles in physical and chemical atmospheric processes, it has been extensively used in laboratory experiments to  
understand and reproduce these processes. In the past 20 years, more than 200 articles have been published using AS as (seed)

30 particles for the study of optical properties, hygroscopic properties, phase transition and viscosity, as well as chemical reactivity  
of aerosols (see the detailed references in SI1). In all these studies, it was shown that the presence of organic matter, even at  
very low concentrations in AS particles, greatly influences these properties.

Among these, the study of aerosol hygroscopic properties represents the major contribution (115 papers out of the  
219 cited in SI1). AS aerosols are very often chosen as seed particles to study hygroscopic behavior of mixed organic-inorganic  
35 aerosols. Scanning various conditions of temperature and relative humidity (RH), hygroscopicity properties of aerosols were  
investigated *via* measurements of hygroscopic growth, cloud condensation nuclei (CCN) activity and ice nuclei (IN) activity.  
It is well established that the hygroscopic parameter kappa ( $\kappa$ ) of pure AS particles is 0.53 [0.33 - 0.72] and 0.61 according to  
the growth factor derivation and the CCN derivation, respectively (Clegg et al., 1998; Koehler et al., 2006; Petters and  
Kreidenweis, 2007). Laboratory studies show that the hygroscopic behavior of most water soluble inorganic mixed aerosols is  
40 additive in nature, i.e., following the ZSR (Zdanovskii, Stokes, and Robinson) assumption (Stokes and Robinson, 1966).  
However, when organic compounds are present in AS aerosols, their hygroscopic properties are more complex. Firstly, for  
water soluble organic compounds such as short carbon chain (di)carboxylic acids, their effects on AS aerosols are represented  
by their hygroscopicity and mass fraction suggested by the ZSR assumption (Abbatt et al., 2005; Brooks et al., 2004; Hämeri  
et al., 2002; Prenni et al., 2003). Secondly, for less soluble compounds and complex mixtures, their solubility significantly  
45 influences the hygroscopic behavior of AS aerosol. At sub-saturation conditions, secondary organic aerosol (SOA) formed on  
AS seed particles from  $\alpha$ -pinene photo-oxidation lowers the hygroscopic growth factor (HGF) of AS (Meyer et al., 2009).  
Specifically, at RH below the deliquescence point, AS seeded SOA do not follow the ZSR predictions because the solutions  
are highly concentrated and thus non-ideal. When the insoluble organic compounds are the dominant components of the  
aerosol, the water uptake on organic-AS particles is significantly slowed down and requires a longer residence time to achieve  
50 the thermodynamic equilibrium (Sjogren et al., 2007). The same behavior has also been observed at super-saturation  
conditions, i.e., the thick coating of insoluble organics compounds such as stearic acids, act as a shield preventing the  
interaction of AS and water, thus suppressing AS hygroscopicity (Abbatt et al., 2005). Thirdly, it was found that organic  
compounds could affect the hygroscopicity of AS by lowering the surface tension, such as marine organic compounds at low  
concentrations (Moore et al., 2008), or ozonolysis products of monoterpenes (King et al., 2009; Wex et al., 2009; Engelhart et  
55 al., 2008). It has been shown that atmospheric surfactants could reduce the aerosol surface tension by a factor of 2 compared  
to water surface tension ( $72 \text{ mN}\cdot\text{m}^{-1}$ ) (Gérard et al., 2019; Nozière et al., 2014; Sorjamaa et al., 2004). The presence of small  
amounts of surface-active organic compounds may reduce the aerosol surface tension, affecting its hygroscopic properties:  
according to some models, a 10 % reduction of the surface tension results in a 30 % increase of the hygroscopic parameter  $\kappa$   
(Ovadnevaite et al., 2017; Petters and Kreidenweis, 2013). More recently, several models have shown that the inferred behavior  
60 of the surface tension strongly depends on the selected modelling approach (Prisle, 2021; Vepsäläinen et al., 2022). In  
conclusion, organic compounds can have a very complex impact on the hygroscopic growth and CCN activity of aerosol  
particles which may go beyond the simple reduction of the value of a single parameter in the Köhler equation, and numerous  
models are currently under development on this issue.

AS has also been widely used to understand the phase transition of organic-inorganic compounds in single particles  
65 studies (49 papers out of the 219 cited in SI1). Under sub-saturated conditions, deliquescence of pure AS occurs at ~ 80 % RH  
and efflorescence at ~ 34 % RH. However, these phase transition behaviors of AS particles are significantly influenced by  
organic compounds. For example, the presence of humic acids decreases the deliquescence RH and increases the efflorescence  
RH of AS aerosols (Badger et al., 2006). Furthermore, the presence of malonic acid on AS particle leads to a two-step  
deliquescence instead of a single step in the hygroscopic growth (Treuel et al., 2009). Differently to the shift of deliquescence  
70 RH and/or efflorescence RH, the presence of SOA completely removes the clear phase transition of AS on the particle: this  
was clearly shown for SOA derived from cycloalkene photolysis and monoterpenes photo-oxidation (Varutbangkul et al.,  
2006). The change in phase transition behavior of AS particle also depends on the quantity of organic compounds. During the  
hygroscopic growth, for small organic/inorganic ratios (< 20 %), there is a bulk-to-surface partitioning with a part of the  
organic material in solution, and another part as a film coated at the surface of the droplet (Nandy and Dutcher, 2018; Smith  
75 et al., 2013); while high organic/inorganic ratios (> 80 %) induce liquid-liquid phase separation (Smith et al., 2013; Saukko et  
al., 2015).

Due to their hygroscopic properties, AS aerosols easily provide an aqueous environment, where reactions between  
 $\text{NH}_4^+$ ,  $\text{SO}_4^{2-}$  and water-soluble organic compounds can play an important role on the formation of secondary aerosols (62  
papers among the 219 cited in SI1). Some of these reactions may explain the source of the so-called “brown carbon”, thus  
80 affecting the optical properties of particles (44 papers among the 219 cited in SI1). Ammonium cations ( $\text{NH}_4^+$ ) are in a pH-  
dependent equilibrium with dissolved ammonia in the aqueous phase.  $\text{NH}_3$  can react with carbonyl compounds such as glyoxal,  
methylglyoxal, glycolaldehyde, hydroxyacetone, biacetyl or unsaturated dialdehydes in Maillard-type browning reactions to  
form light absorbing and oligomeric compounds such as imidazoles or pyrazine-based compounds (Hensley et al., 2021; Grace  
et al., 2020; Hawkins et al., 2018; Laskin et al., 2014; Kampf et al., 2012). These reactions are of particular interest for the  
85 atmosphere, as they have an impact on both health and climate. Their aqueous-phase processes represent an important and  
rapid source of brown carbon (Powelson et al., 2014; De Haan et al., 2017; Jimenez et al., 2022). In addition,  $\text{SO}_4^{2-}$  is not inert  
in atmospheric water. Sulfate anions can react with  $\cdot\text{OH}$  radicals forming sulfate radicals ( $\text{SO}_4^{\cdot-}$ ), an important atmospheric  
oxidant (Herrmann, 2003). Besides, sulfate radicals contribute to the formation of organosulfates (Nozière et al., 2010;  
Brüggemann et al., 2020; Wach et al., 2019; Szmigielski, 2016). Organosulfates are ubiquitous compounds in SOA with  
90 important implications in their physicochemical properties (Shakya and Peltier, 2015). Other chemical pathways that lead to  
the formation of organosulfates might involve directly sulfate anions, i.e., their nucleophilic substitution to epoxides or tertiary  
nitrates (Hu et al., 2011; Darer et al., 2011), and the acid-catalyzed esterification of alcohol groups (Surratt et al., 2008; Iinuma  
et al., 2007).

Due to the atmospheric representativity of AS particles and their well-known physical and chemical properties, they  
95 are often chosen as a reference in aerosol studies, as mentioned above, and for instrumentation calibration. The presence of  
trace organic compounds in AS particles may induce potentially important artefacts on the experimental results of physical  
and chemical processes. Few laboratory studies show that organic compounds can be present in synthetic AS particles. For

example, 0.8 wt % of C was observed in solutions where only ammonium sulfate was present as solute in the study of phase transitions of AS (Badger et al., 2006). Another example, in a study of glyoxal uptake on AS particles monitored by an Aerosol Mass Spectrometer, Trainic et al., (2011) found organic fragments on pure AS aerosols (purity not mentioned), with an organic/sulfate ratio as high as 8 %. Scanning the 219 articles (mentioned in SI1) published over the last 20 years using AS aerosols in the laboratory, it appeared that neither quantification nor identification of these potential organic impurities was reported. Furthermore, the majority of these studies (63 %) did not mention the origin and purity of AS used. As organic traces may significantly influence the properties of AS particles, and thus bias experimental results, the objectives of this work were to quantify organic traces in commercial AS under conditions used in laboratory experiments, and when possible, tentative identification was performed. Finally, recommendations are given for purity improvements.

## 2 Method

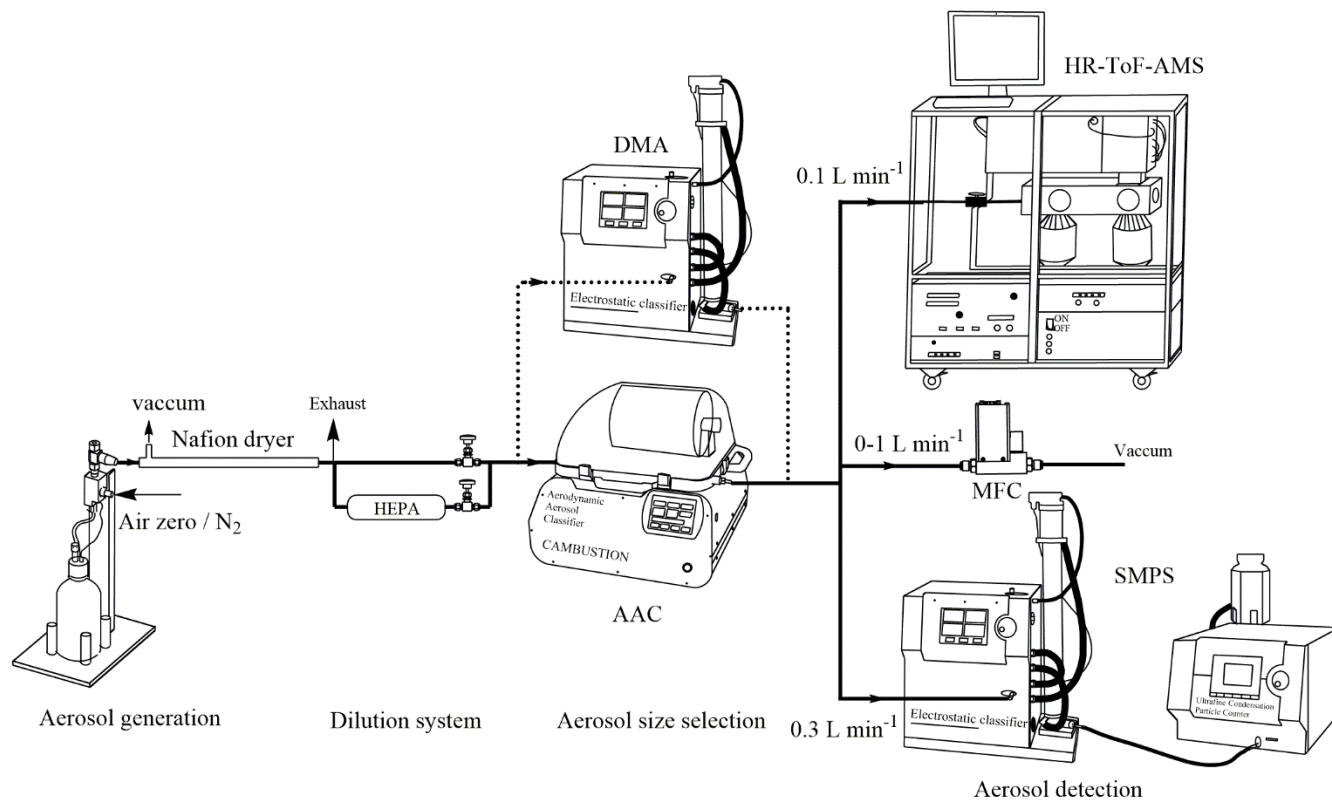
AS aerosol particles were generated by atomization of AS solutions at concentrations ranging from 0.01 to 0.5 M. AS aerosols were selected at 4 sub-micrometer sizes to test the effect of particle size on the organic content. This procedure allowed us to form quasi-monodisperse AS particles at mass concentrations ranging from 5 to 30  $\mu\text{g m}^{-3}$ , concentrations typically used for aerosol generation and/or calibration in the literature. Their chemical composition was quantified on-line by a high-resolution time-of-flight aerosol mass spectrometer (HR-ToF-AMS). Additionally, aqueous solutions of AS were analyzed by Liquid Chromatography–tandem Mass Spectrometry (LC-MS) to tentatively identify organic content. All chemical compounds used in this work are listed in SI2.

### 2.1 Detection of organic traces in AS aerosol particles

#### 2.1.1 Aerosol generation and size classification

The schematic of the experimental setup for quantifying organic content is shown in Fig. 1. Aqueous solutions of AS (0.01 - 0.5 M) were nebulized by atomization (using a TSI, 3076 atomizer) that generated droplets with compressed air at 1 bar above atmospheric pressure and a flowrate of 1.8  $\text{L}\cdot\text{min}^{-1}$ . As a comparison with compressed air, pure  $\text{N}_2$  (Linde Gas, 99.999 %) was used. The resulting droplets were dried by a Nafion™ dryer at relative humidity (RH) below 25 %, i.e., below the efflorescence of AS aerosol. Dry AS particles then passed through a dilution system aimed at controlling AS particle concentrations. It consisted of two parallel pathways, one of which was connected to a HEPA filter. An aerodynamic aerosol classifier (AAC, Cambustion) and an electrostatic classifier (TSI, 3080) combined with a differential mobility analyzer (3081 long DMA) were alternatively used to select monodisperse particles. The sheath/sample air flow ratio was fixed at 10 for the two classifiers. To regulate the flowrate through the AAC classifier, a mass flow controller (MFC) was connected to a vacuum pump. Under this configuration, the sample flow through the AAC varied from 0.4 to 1.4  $\text{L}\cdot\text{min}^{-1}$ , while the tests performed with the DMA classifier were only done at one flowrate (0.4  $\text{L}\cdot\text{min}^{-1}$ ). This setup allowed the characterization of the aerosol

particles by their sizes, as well as their organic content as a function of particle sizes with respect to the total mass of AS particles selected.



130

**Figure 1.** Experimental setup for the quantification of organic content in monodisperse ammonium sulfate particles.

### 2.1.2 Experimental conditions for the investigation of AS aerosol particles

A series of experiments (Table 1) was performed to quantify organic content on AS aerosol particles by scanning various conditions of mass concentrations, particle size, and generation procedures. In this work, four different particle diameters were used: the mobility diameter ( $d_m$ ), the aerodynamic diameter ( $d_a$ ), and the vacuum aerodynamic diameter ( $d_{va}$ ) were given by the SMPS, the AAC and the AMS measurements, respectively; while the volume equivalent diameter ( $d_{ve}$ ) was used to determine the surface of AS particle. The relations between these diameters were described by DeCarlo et al., (2004). As organic compounds can be homogeneously mixed in AS aerosol or remain at particle surface inducing different behavior as a function of size (Jimenez et al., 2009; Tervahattu et al., 2002), monodisperse AS particles were selected with aerodynamic size ( $d_a$ ) varied from 200 nm to 500 nm in each experiment. In experiment P1 (EXP P1), AS crystals (99.5 %, for analysis, from ACROS Organics™ Fisher Scientific) were dissolved in Milli-Q water (18.2 MΩ.cm<sup>-1</sup>, TOC < 2ppb) at various concentrations (0.01 - 0.5 M). In EXP P2 to P7, the aqueous phase concentration of AS was fixed at the highest value (0.5 M) to study the influence of other parameters. In EXP P2, the influence of the water quality was tested. In EXP P3 to P5, the

140

influence of the purity of AS crystals was tested. In EXP P3, AS crystals (99.5 %, for analysis, from ACROS Organics™  
 145 Fisher Scientific) were tentatively purified by an Accelerated Solvent Extractor (ASE 300, Dionex) using acetonitrile as  
 extraction solvent. In EXP P4, AS crystals (99.5 %, for analysis, from ACROS Organics™ Fisher Scientific) were tentatively  
 purified by recrystallization in Milli-Q water: AS crystals (20 g) were dissolved into boiling water (20 mL) reaching a  
 concentration of 7.5 M and then recrystallized by smooth cooling at room temperature. In EXP P5, high purity AS (99.9999%  
 Suprapur® from Merck) was used. In EXP P6, the influence of the particle size selector was studied by inter-comparison  
 150 between the DMA and the AAC. Developed by Tavakoli and Olfert (2013), the AAC is a recent commercial aerosol classifier  
 which selects the particle size by centrifugal force instead of electrostatic force which is used in the DMA. In the AAC, the  
 aerodynamic diameter of selected particles is related to the rotational speed of the concentric cylinder, the sheath flow rate and  
 the sample flow rate. Rotational speed has been reported to influence the geometric standard deviation ( $\sigma_{\text{geo}}$ ) of size  
 distribution, i.e., the higher the rotational speed, the smaller the size and the larger the  $\sigma_{\text{geo}}$  (Johnson et al., 2018). In EXP P7,  
 155 the effect of the rotational speed of the concentric cylinder in the AAC was tested while maintaining a constant size selection  
 by regulating the MFC (Fig. 1), so that the sample flow through the AAC varied from 0.4 to 1.4 L.min<sup>-1</sup>.

**Table 1.** Experiments to quantify organic traces on AS aerosol particles under various conditions: <sup>(1)</sup> AS 99.5%, for analysis, from ACROS  
 Organics™ Fisher Scientific; <sup>(2)</sup> purification by solvent (acetonitrile) extraction; <sup>(3)</sup> purification by recrystallisation; <sup>(4)</sup> AS 99.9999%  
 160 Suprapur® from Merck. <sup>(5)</sup> Milli-Q water, 18.2 M $\Omega$ .cm<sup>-1</sup>, TOC < 2 ppb; <sup>(6)</sup> Fisher Chemical, LC-MS Grade. Under each condition, duplicate  
 experiments were performed for each selected particle size. The four sizes ( $d_a = 200, 300, 400$  and  $500$  nm) selected with the AAC classifier  
 correspond to the mobility sizes ( $d_m = 130, 201, 269$  and  $336$  nm)

Experiment	AS purity %	water	AS liquid concentration (M)	Particle size (nm)
Size selection by the AAC (sample flow = 0.4 L.min <sup>-1</sup> )				
P1	99.5 <sup>(1)</sup>	Milli-Q <sup>(5)</sup>	0.01, 0.02, 0.05, 0.1, 0.2, 0.5	$d_a = 200, 300, 400, 500$
P2	99.5 <sup>(1)</sup>	Fisher <sup>(6)</sup>	0.5	$d_a = 200, 300, 400, 500$
P3	99.5 <sup>(1)</sup> purified <sup>(2)</sup>	Fisher <sup>(6)</sup>	0.5	$d_a = 200, 300, 400, 500$
P4	99.5 <sup>(1)</sup> recryst <sup>(3)</sup>	Fisher <sup>(6)</sup>	0.5	$d_a = 200, 300, 400, 500$
P5	99.9999 <sup>(4)</sup>	Fisher <sup>(6)</sup>	0.5	$d_a = 200, 300, 400, 500$
Size selection by the DMA (sample flow = 0.4 L.min <sup>-1</sup> )				
P6	99.5 <sup>(1)</sup>	Milli-Q <sup>(5)</sup>	0.5	$d_m = 122, 188, 250, 311, 375$
Size selection by the AAC (sample flow = 0.5, 1.0, 1.4 L.min <sup>-1</sup> , corresponding to rotation speed of 190, 285 and 369 rad/s)				
P7	99.5 <sup>(1)</sup>	Milli-Q <sup>(5)</sup>	0.5	$d_a = 300$
Effect of gas supplier (pure N <sub>2</sub> instead of compressed air)				
P8	99.5 <sup>(1)</sup>	Milli-Q <sup>(5)</sup>	0.5	$d_a = 200, 300, 400, 500$

### 2.1.3 Characterization of aerosol particles

165 The particles number size distribution was measured with a scanning mobility particle sizer (SMPS) consisting of a DMA (TSI, 3080) coupled with an Ultrafine Condensation Particle Counter (CPC, 3776, TSI). A high-resolution time-of-flight aerosol mass spectrometer (HR-ToF-AMS, Aerodyne Research) was used to measure the bulk chemical composition of non-refractory submicron particulate matter (DeCarlo et al., 2006). The instrument was used under standard conditions (standard vaporizer at 600 – 650 °C and electron ionization at 70 eV) in V-mode and in p-ToF mode. Each measurement point was  
170 averaged for MS cycle of 1 min and p-ToF cycle of 30 s. Calibrations using pure and dried particles of ammonium nitrate and ammonium sulfate with a mobility diameter of 350 nm was carried out every few days of operation to determine the Ionization Efficiency of nitrate, ammonium and sulfate named as  $IE_{NO_3}$ ,  $RIE_{NH_4}$  and  $RIE_{SO_4}$ . The  $RIE_{NH_4}$  and  $RIE_{SO_4}$  values were related to nitrate and were estimated experimentally as 3.3 and 1.8, respectively. The standard recommended value for  $RIE_{org}$  of 1.4 was used for organic compounds. Calibration in p-ToF mode was carried out using pure ammonium nitrate in the size range  
175 80-500 nm mobility diameter. The data treatment has been performed with AMS Analysis Toolkit 1.63 and PIKA 1.23 under the software Igor Pro 6.37. The selection of ions to fit in PIKA was derived from the mass spectra produced by AS aerosols at  $d_a = 200$  nm in EXP P1 and was re-checked in each experiment. To avoid any over-estimation of the organic fraction,  $CHO^+$  and  $CO_2^+$  fragments (at  $m/z$  29 and 44) were corrected from the remaining gas phase in the AMS (Aiken et al., 2007; Canagaratna et al., 2015). In addition, due to the very high signals of the fragments  $NH_x$  and  $SO_x$ , other fragments located at  
180 the tail of these main peaks (such as  $CH_3^+$ ,  $CH_4^+$ ,  $CH_2N^+$  and  $C_2H_4^+$ ...) were excluded from the calculation of the total organic content, to avoid any over-estimation of the organic fraction.

### 2.2 Seeking for organic traces in AS aqueous solutions

The characterization of organic traces on AS aerosol particles were also investigated directly in AS aqueous solutions using a Liquid Chromatography–tandem Mass Spectrometer (LC-MS) for tentative molecular identification. The system  
185 comprised liquid chromatograph (Acquity system, Waters) coupled with Quadrupole-Time-of-Flight Mass Spectrometer (Synapt G2 HDMS, Waters) fitted with an electrospray ion source (ESI). The chromatographic separation was carried out on an Atlantis T3 reversed phase C18 column (100\*2.1; 3  $\mu$ m, Waters), the mobile phase consisted of two eluents: eluent A was Milli-Q water (resistivity 18  $M\Omega \cdot cm^{-1}$  at 25 °C) with 0.1 % formic acid, and eluent B was either methanol (Optima<sup>®</sup> LC/MS grade, Fisher Scientific) with 0.1 % formic acid or acetonitrile (Fisher Chemical, Optima<sup>®</sup> LC/MS grade) with 0.1 % acid. The  
190 gradient elution was performed at a flow rate of 0.4 mL  $min^{-1}$  using 5 % of (B) held 1 min and 5 – 95 % of (B) within 5 min. The sample injection volume was 5  $\mu$ L. In the ESI, the capillary voltage was set to 1 kV, the desolvation gas flow was 1000 L.h<sup>-1</sup> at 500 °C and the source temperature was 150 °C. During each chromatographic run, leucine enkephalin (2 ng. $\mu$ L<sup>-1</sup>,  $C_{28}H_{37}N_5O_7$ , molecular weight 555.27 g.mol<sup>-1</sup>, Sigma-Aldrich) was used as internal standard to perform mass correction. The mass spectrometer was tuned to V-mode with a resolving power of 18000 at  $m/z$  400 and allowed the determination of  
195 elemental composition with a mass accuracy lower than 5 ppm. For elemental attribution, the ranges of atom number were set

as follows: C [0-30], H [0-60], N [0-5], O [0-10], S [0-3], P [0-3], Na [0-1] thus covering the most common elements (Kind and Fiehn, 2007). An isotope prediction algorithm, based on the mass of the molecular ion and the relative intensity of the 1<sup>st</sup> and 2<sup>nd</sup> isotopes, was applied to reduce the number of proposed elemental compositions. Data were collected from 50 to 600 Da in the positive and negative ionization modes. All products were detected as their protonated molecules ( $[M+H]^+$ ) or sodium adducts ( $[M+Na]^+$ ) in the positive mode, and their deprotonated molecules ( $[M-H]^-$ ) in the negative mode. In some experiments, complementary analyses were performed using MS/MS fragmentation with various collision energies.

Although the organic purity is not mentioned on commercial crystals (only the inorganic content is indicated), two different brands of AS of the same purity were analyzed to seek for potential organic traces and for comparison purposes: one from ACROS Organics™ Fisher Scientific (99.5 %, for analysis) that has been widely used in the literature and one EMSURE® from Merck (99.5 %, for analysis). The characterization experiments are shown in Table 2, each one was systematically complemented by blank experiments, i.e., analysis of the water used for each AS solution.

Table 2: Experiments of characterization of organic traces in AS liquid solutions. The elution gradient and ESI setup were the same for all experiments. <sup>(1)</sup> AS 99.5%, for analysis, from ACROS Organics™ Fisher Scientific; <sup>(2)</sup> AS 99.5% EMSURE® from MERCK <sup>(3)</sup> Eluents: A= H<sub>2</sub>O with 0.1% formic acid, and B as specified; <sup>(4)</sup> acetonitrile, <sup>(5)</sup> methanol, <sup>(6)</sup> methyl tert-butyl ether, <sup>(7)</sup> dichloromethane. L-L: liquid-liquid, S-L: solid-liquid.

Experiment	Type of experiment				LC-MS analytical conditions	
	AS purity %	AS aqueous concentration	Sample preparation	Extracting solvent	Eluent B <sup>(3)</sup>	MS Mode
C1	99.5 <sup>(1)</sup>	1.5 M	None	-	ACN <sup>(4)</sup> 0.1% acid	ESI <sup>+</sup> -MS/ ESI-MS
C2					MeOH <sup>(5)</sup> 0.1% acid	
C3					L-L extraction	MTBE <sup>(6)</sup>
C4		DCM <sup>(7)</sup>				
C5		2.5 M	ACN <sup>(4)</sup>			
C6						
C7		crystals	S-L extraction	MeOH <sup>(5)</sup> 0.1% acid		
C8					99.5 <sup>(2)</sup>	
C9		99.5 <sup>(1)</sup>	5 M	L-L extraction		ESI <sup>+</sup> -MS-MS



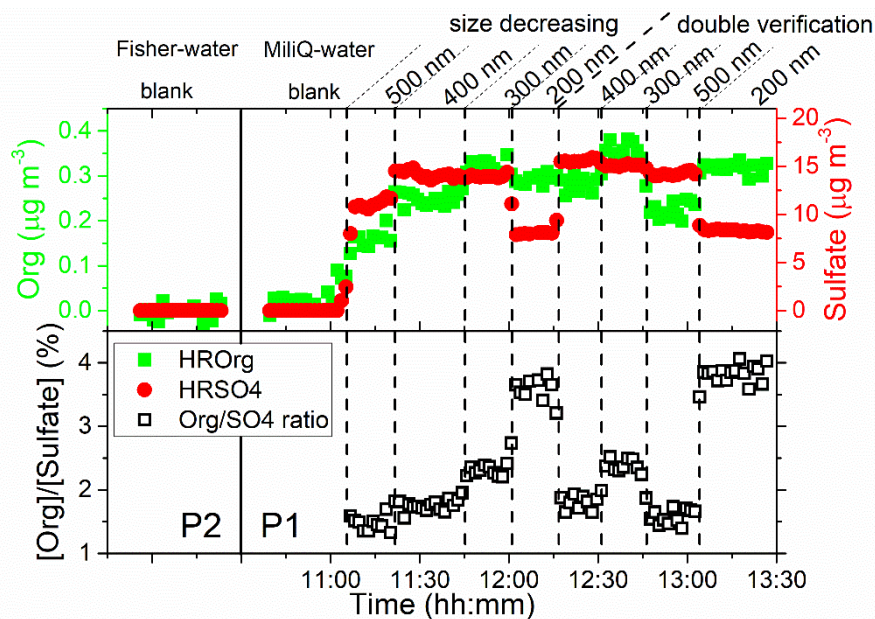
C10	99.5 <sup>(2)</sup>	5 M	L-L extraction			ESI <sup>+</sup> -MS / ESI-MS
-----	---------------------	-----	-------------------	--	--	----------------------------------

In EXP C1 and C2, aqueous solutions of AS were injected into the LC-MS, and two elution solvents were tested to optimize the chromatographic separation. In EXP C3 to C10, organic compounds were extracted from AS crystals by different methods (solid-liquid and liquid-liquid extraction) using various solvents, and preconcentrated prior LC-MS analysis using both positive and negative modes. For these extractions, an Accelerated Solvent Extractor (ASE 300, Dionex) system was used under the following conditions: acetonitrile was the extraction solvent, the oven was set at 100 °C under 100 bars, the heat up time and static time were 5 min each, three extraction cycles were conducted. As an extension of EXP C6, EXP C9 was designed to perform MS/MS analysis using very high concentrations of AS to optimize the identification of organic traces, and analysis were performed in the positive mode only. For comparison purposes, another brand of AS of the same purity (99.5 %) were used in EXP C8 and C10 using two extraction methods.

### 3 Results and discussions

#### 3.1 Organic content on AS aerosol particles

A significant quantity of organic matter was directly observed by the HR-ToF-AMS in EXP P1. As an example, Figure 2 shows the mass concentrations of total organic matter and sulfate and their ratios as a function of time during one size cycle performed in EXP P1 at AS concentration of 0.01 M. Figure 2 also provides background signals obtained with the two pure waters of different qualities used in EXP P1 and P2. In these background signals, the total mass concentrations of organic compounds and sulfate are  $0.018 \pm 0.009 \mu\text{g}\cdot\text{m}^{-3}$  and  $0.002 \pm 0.001 \mu\text{g}\cdot\text{m}^{-3}$ , respectively, similar to the detection limits of the HR-ToF-AMS in the V mode (DeCarlo et al., 2006). In the presence of AS, a significant quantity of organic compounds was observed with concentrations ranging from 0.15 to  $0.33 \mu\text{g}\cdot\text{m}^{-3}$  when aerodynamic size of the particle varied from 500 nm to 200 nm, with a very good reproducibility in the duplicate experiments, at each size. Furthermore, the evolution of the mass ratio between total organic compounds and sulfate marked as [Org]/[Sulfate] (Fig. 2) shows a clear correlation with particle size: this ratio increases when the particle size decreases. The same observations were obtained at all other AS concentrations investigated in EXP P1 and in the other experiments. It was checked in EXP P8 that replacing compressed air by pure N<sub>2</sub> (Linde Gas, 99.999 %), no significant differences were observed from EXP P1 under the same conditions (SI3). Overall, it was observed that [Org]/[Sulfate] varied from 1.5 % to 3.8 %, in the range of the values reported by studies mentioning the presence of organic compounds in laboratory experiments on AS particles (0.8 wt % of C in Badger et al., 2006 and up to 8% in Trainic et al., 2011).



240

**Figure 2:** Mass concentrations of total organic matter, sulfate and organic/sulfate ratio as a function of time during one cycle performed in EXP P1 at AS concentration of 0.01 M. Background signal obtained with pure water in EXP P1 and P2 is also shown for quality check and for comparison between the two types of water with different purity.

245 The total mass concentration of organic compounds was calculated based on all organic fragments, as described in the previous Sect 2.1.3. Figure 3 shows the Unit-mass resolution spectrum of AS aerosols selected by the AAC at  $d_a = 200$  nm.

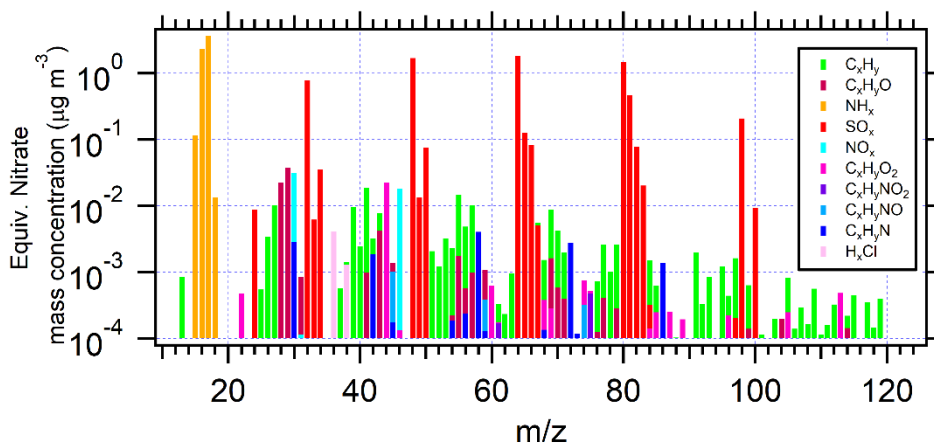


**Figure 3 :** Unit-mass resolution spectra (averaged over 12 measurements, converted from the high-resolution data) of AS aerosol particles ( $d_a = 200$  nm) in EXP P1, performed at AS concentration of 0.5 M.

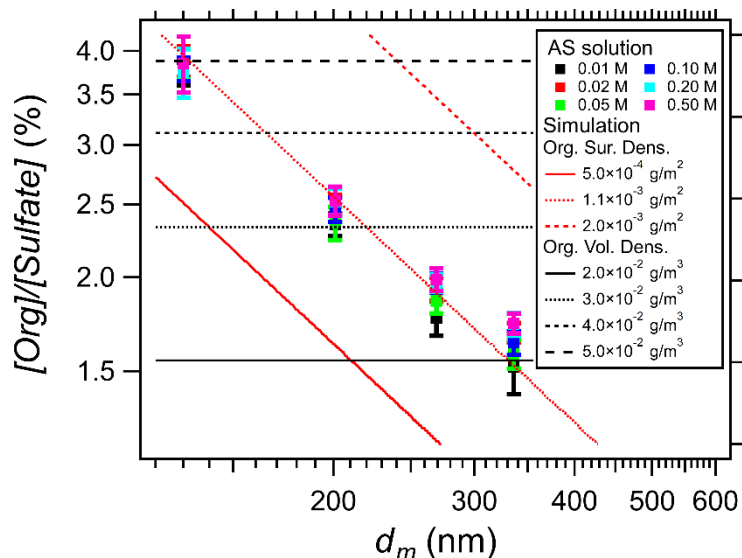
250

$\text{SO}_x$  and  $\text{NH}_x$  families represent sulfate and ammonium, respectively. All the other fragments are between 1 and 3 orders of magnitude lower, but detectable signals span for  $m/z$  up to 100. The sum of the signals of  $\text{NO}_2^+$  and  $\text{NO}^+$  fragments

represent 30% of the total organic signal (Fig. SI4-2). To figure out the source of this non-negligible nitrate signal, the AMS signal  $\text{NO}_2^+/\text{NO}^+$  ratio was investigated and showed significantly lower values in AS aerosol (0.46 in EXP1) compared to ammonium nitrate particles used for calibration (1.18) – Fig. SI4-1. It is thus suggested that the observed nitrate signal in AS aerosol is due to the presence of organic nitrates (Kiendler-Scharr et al., 2016). Concerning organic fragments, significant signals were observed for fragments  $\text{C}_x\text{H}_y^+$  at  $m/z$  27, 39, 41, 43, 55, 57, 67, 69, for  $\text{C}_x\text{H}_y\text{O}^+$  at  $m/z$  of 28 and 30, for  $\text{C}_x\text{H}_y\text{O}_2^+$  at  $m/z$  44, for  $\text{C}_x\text{H}_y\text{N}^+$  at  $m/z$  30, 58, 72, 86 (raw spectra of CHN fragments are shown in SI5). The potential “Pieber effect” was also investigated to elucidate any positive artefact on the determined quantities of organic compounds. Indeed, Pieber et al., 2016 showed that inorganic salts like AS or ammonium nitrate can trigger the  $\text{CO}_2^+$  signal ( $m/z$  44) due to reactions on the vaporizer of the AMS instrument. In the present study, the observed  $\text{CO}_2^+$  signal represented  $20 \pm 5$  % of the total organic signal. Thus, if all the  $\text{CO}_2^+$  fragments came from the interference signal of sulfate, the maximum Pieber effect in this work would be 0.76 % relative to sulfate. It was thus not considered in the results. The rest of the organic fragments seem to represent organic molecules bearing various functionalities, potentially comprising oxygen and nitrogen. Before further identification of these compounds, Sect 3.2 and Sect 3.3 present the results and discussions on the influence of the particle size and liquid AS concentrations on the organic content.

### 3.2 The role of particle size and liquid AS concentrations on the quantity of organic content

Figure 4 shows the  $[\text{Org}]/[\text{Sulfate}]$  measured in AS aerosols at various nebulized solution concentrations as a function of particle size. While no significant influence of AS aqueous phase concentration has been found (within experimental uncertainty), a significant influence of particle size is clearly observed on the  $[\text{Org}]/[\text{Sulfate}]$ .



270

**Figure 4 :** Organic/sulfate mass concentration ratios in AS aerosols versus particle mobility size ( $d_m$ ) during EXP P1 scanning the six nebulized AS concentrations (0.01 to 0.5 M). The colored dots (with error bars) are the experimental data, while the red and black lines represent the calculated  $[\text{Org}]/[\text{Sulfate}]$  considering either surface coating of organic matter (in red from Eq. 3) or internal mixing (in black from Eq. 4)

275 To further understand how the organic matter was mixed with AS aerosols, two series of calculations were performed, following two hypotheses on the organic-inorganic mixing: i) organic coating on the surface of monodisperse AS particles, and ii) internal mixing. To achieve this calculation, a thorough study of the morphology of AS particles was performed using the various sizes measurements (Appendix A). For monodisperse AS particles selected by the AAC at a required aerodynamic diameter ( $d_a$ ), its mobility diameter ( $d_m$ ) and vacuum aerodynamic diameter ( $d_{va}$ ) were measured by SMPS and HR-ToF-AMS, respectively.

280 The calculations of the organic-sulfate ratio using each of these two hypotheses are detailed hereafter:

- Hypothesis 1: AS aerosols were coated by organic compounds with a size-independent surface density  $\rho_{org,S}$  (in  $\text{g}\cdot\text{m}^{-2}$ ).

For non-spherical particle, the total surface of particle was considered as the surface of volume equivalent particle. According to DeCarlo et al., (2004), the relation between volume equivalent diameter ( $d_{ve}$ ) and  $d_a$  is described as Eq. 1:

$$d_a = d_{ve} \sqrt{\frac{\rho_p}{\rho_0} \frac{1}{\chi} \frac{C_c(d_{ve})}{C_c(d_a)}} \quad (1)$$

Where  $\chi$  is the shape factor of aerosol particles and  $C_c$  is the Cunningham slip factor (Kim et al., 2005), given by Eq. 2.

$$C_c(K_n) = 1 + K_n \left[ 1.165 + 0.483 \exp\left(-\frac{0.997}{K_n}\right) \right] \quad (2)$$

$K_n(d) = 2\lambda_g/d$  is the Knudsen number, and  $\lambda_g$  is the gas mean free path. In this work,  $d_a$  was given by the AAC;  $\chi$  was determined by  $d_m$  and  $d_{va}$  (Appendix A). Normal temperature and pressure (293.15 K at 1 atm) were applied for the calculation of  $d_{ve}$ . The surface of AS particles was estimated from the value of  $d_{ve}$ . Therefore, the prediction of surface coated organic compounds compared to sulfate mass is described in Eq. 3.

$$\frac{[Org]}{[Sulfate]} = \frac{\rho_{org,S} S_{ve}}{V_{ve} \rho_{AS} \frac{M_{SO_4}}{M_{AS}}} = \frac{3}{2} \frac{\rho_{org,S}}{d_{ve} \rho_{AS}} \frac{M_{SO_4}}{M_{AS}} \times 100\% \quad (3)$$

Where  $S_{ve}$  and  $V_{ve}$  are the surface and volume of the volume equivalent AS particle, respectively.  $M_{SO_4}$  and  $M_{AS}$  are molar mass of  $\text{SO}_4^{2-}$  and  $(\text{NH}_4)_2\text{SO}_4$ , respectively. [Org] and [Sulfate] are the mass concentrations of organic compounds and of sulfate in the particulate phase. Eq. 3 shows that, in this case, the ratio [Org]/[Sulfate] decreases when the particle size increases.

- Hypothesis 2: Organic compounds are homogeneously mixed in AS aerosols with an density  $\rho_{org,V}$  (in  $\text{g}\cdot\text{m}^{-3}$ ). In this case, the mass concentrations of organic compounds compared to sulfate is described by Eq. 4.

$$\frac{[Org]}{[Sulfate]} = \frac{V\rho_{org,V}}{V\rho_{AS}\frac{M_{SO_4}}{M_{AS}}} = \frac{\rho_{org,V}}{\rho_{AS}\frac{M_{SO_4}}{M_{AS}}} \times 100\% \quad (4)$$

300 Where  $V$  is the total volume of studied aerosol particle. In this case, the ratio  $[Org]/[Sulfate]$  is independent of the particle size.

The results of these two calculations are shown in Fig. 4 together with the experimental results. The comparison clearly shows that the organic compounds coat homogenously on the surface of AS particles with a surface density of  $1.1 \times 10^{-3} \text{ g.m}^{-2}$ . In addition, this result also shows that the Nafion™ dryer was not efficient in removing these organic compounds, probably due to their low volatility.

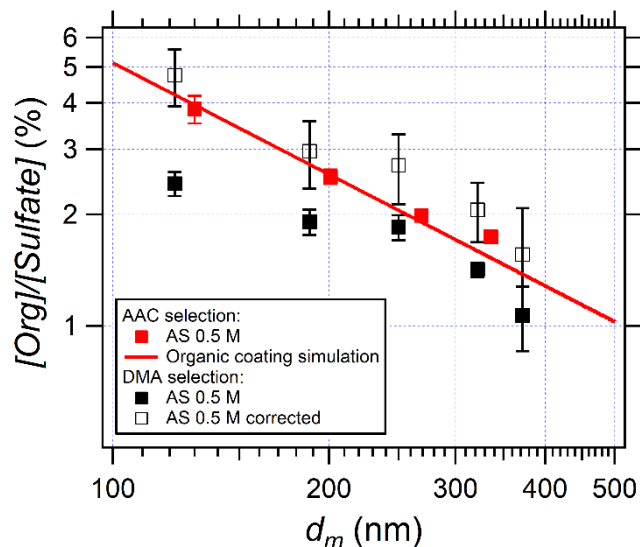
305

### 3.3 Influence of AAC and DMA on the organic content

Particle size selection is important in aerosol science especially when particle size influences the properties studied. In this work, both AAC and DMA were used to provide monodisperse AS aerosols. As a recent commercial instrument, AAC was used to select AS aerosols in most of the experiments. The effects of the concentric cylinder rotation speed of the AAC were tested in EXP P7. The results (SI6) demonstrate that the rotation speed does not affect the  $[Org]/[Sulfate]$ . While the AAC selects particles using centrifugal force, the DMA selects particles by their electromobility. In the latter, the selected distribution is thus not exclusively monodispersed as it contains double- and triple-charged particles at the corresponding sizes. Corrections of the multi-charge effect were successfully applied following the and is routine in aerosol size distribution determination (Petters, 2018; Wiedensohler et al., 2012). However, Figure 4 shows that the larger particle the lower content of the organic compounds. In this case, the multi-charged particles affect the organic quantification using the DMA and the AMS, so that corrections are needed to do. In this work, we compared  $[Org]/[Sulfate]$  in AS particles selected by the DMA and by the AAC, respectively (Fig. 5).

310

315

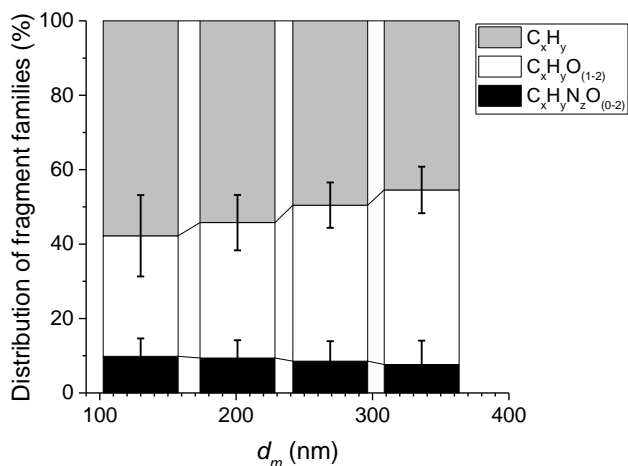


320 **Figure 5** : Influence of instrumental conditions and instrument inter-comparison: AAC selection (red squares, EXP P1), DMA selection (black squares, EXP P6) and multi-charging correction (white squares). The red line represents the calculation simulating organic coated at the AS particle surface using Eq. 3 with a surface density of  $1.1 \times 10^{-3} \text{ g.m}^{-2}$  (selected from Fig. 4).

The white squares represent the multi-charging corrections considering the hypothesis that organic compounds coat the surface of AS particles as shown in Sect 3.2. Details of the multi-charging corrections are given in SI7. Briefly, the corrected  
 325 [Org]/[Sulfate] by the multi-charged modes are systematically higher than the non-corrected values because the correction considers the total amounts of organic compounds and sulfate. Using the DMA selection after correction, the [Org]/[Sulfate] is clearly inversely related to the mobility size and in very good agreement with those obtained using the AAC selection. In conclusion, the intercomparison of the two instruments shows that the influence of the instrument is negligible, and it also shows that the selection by AAC leads to lower uncertainties on the y axis and therefore more accurate results.

### 330 **3.4 Tentative Identification of organic content**

From the HR-ToF-AMS mass spectra, the three main families present in AS particles were  $\text{C}_x\text{H}_y$ ,  $\text{C}_x\text{H}_y\text{O}_{(1-2)}$  and  $\text{C}_x\text{H}_y\text{NO}_{(0-2)}$ . Figure 6 shows the proportion of these three groups relative to total organic compounds as a function of AS particle size. Within the uncertainties, the proportion of the three families remains constant and independent on the particle size, which shows the stability of the organic compounds coated on AS particles.



335

**Figure 6:** Mass fractions of the three main sets of organic fragments present in AS particles as measured by the HR-ToF-AMS during EXP P1. The error bars represent the standard deviation from averaging multiple measurements.

The identification of the corresponding organic compounds was limited by the high fragmentation due to the electron  
 340 impact ionization operated in the HR-ToF-AMS instrument. Further identification was conducted by LC-MS with liquid AS  
 solutions. In EXP C1 and C2, an aqueous solution of ammonium sulfate (99.5 %) at 1.5 M was injected and analyzed in the  
 positive mode. The acetonitrile and methanol eluents showed similar results for compound separation. Figure 7 shows a  
 chromatogram of an ammonium sulfate solution (green line) as well as blanks of Milli-Q water (red line) and Fisher water  
 (blue line). In Milli-Q water, two ions were present at retention times 4.45 min and 4.65 min, their mass spectra were attributed  
 345 as nylon polymers ( $C_6H_{11}NO$ )<sub>n</sub> which are among the frequently reported interfering compounds (Tran and Doucette, 2006;  
 Keller et al., 2008). However, no significant contamination was observed in the Fisher water (LC-MS Grade). Figure 7 shows  
 that the same ions found in Milli-Q water were also present in the AS solution prepared in the same Milli-Q water. Many other  
 ions were detected in the AS solution, and their retention times highly suggested that these molecules were organic. The  
 proposed raw formulas systematically contained carbon, hydrogen, oxygen, nitrogen and sometimes sulfur, consistent with the  
 350 HR-ToF-AMS spectra. The double bond equivalence (DBE) varies from 1 to 5 showing that the molecules are unsaturated and  
 potentially cyclic. Different to nylon polymers found in Milli-Q water, these raw formula are not referenced among the  
 common laboratory LC-MS contaminants (Keller et al., 2008). The mass error was always well below 5 ppm and no raw  
 formula with sodium adduct was suggested. Some of the  $m/z$  showed two different retention times, implying potentially the  
 presence of isomers. For example, at  $m/z$  226.1918, two peaks were detected, one at 2.89 minutes and the other at 3.11 minutes  
 355 as described in detail in SI8 for the most intense ions. In the negative ESI mode, the signal was overwritten by the sulfate ion  
 (detected at  $[M+H]^-$ : 96.9596,  $HSO_4^-$ ) along the whole chromatogram, due to the high ammonium sulfate concentrations used.

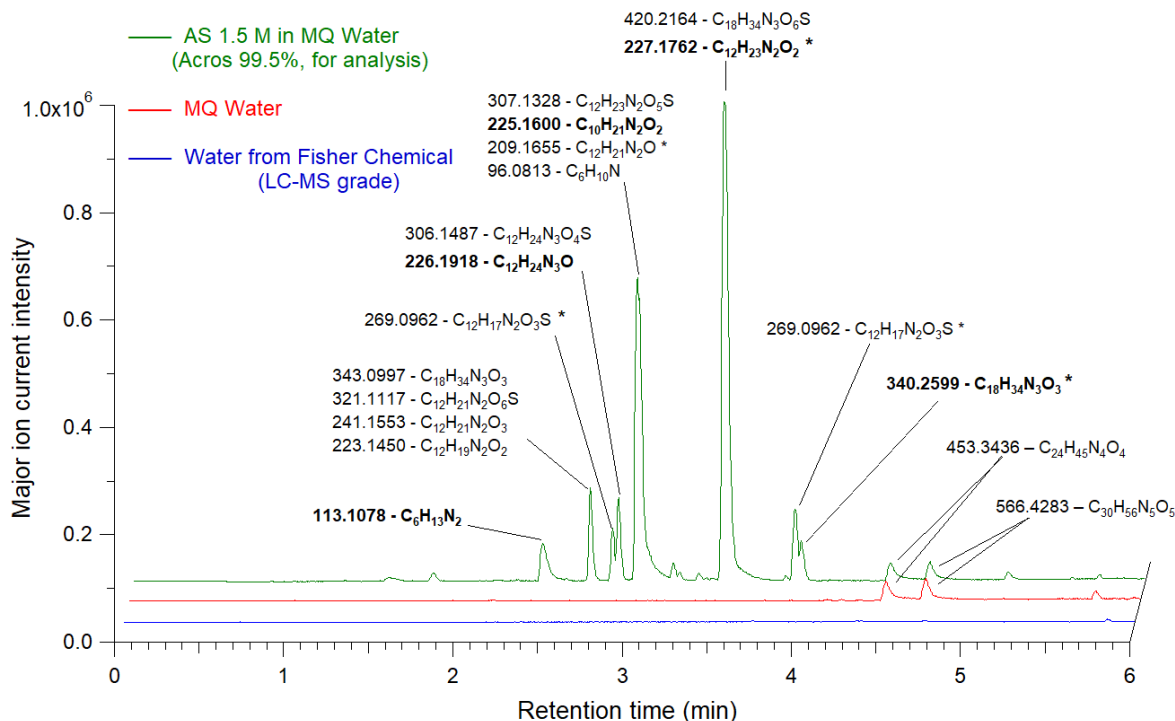


**Figure 7:** LC/ESI<sup>+</sup>-MS base peak chromatogram of Milli-Q water, Fisher water and AS (99.5 %) solution of 1.5 M (EXP C1) with corresponding major ion masses associated with raw formulas. The bold ion masses and proposed raw formula were studied in MS-MS (EXP C9). Ions marked with \* were detected in their [M-H]<sup>-</sup> form in LC/ESI-MS (in EXP C6-8).

For further identification and for detection in the negative mode, AS crystals and solutions at various concentrations were extracted using different solvents and different methods (C3-7 in Table 2). In the positive mode, more than 60 % of the molecules identified without the extraction step were also detected. Compared to other solvents, acetonitrile was found to be the most efficient extracting solvent. In the negative mode, the signal was systematically much lower (ion current intensity < 10<sup>3</sup> counts per second) and only molecules marked with \* in Fig. 7 were detected. Consequently, no further analysis was performed in the negative mode due to the low signal. In EXP C8 and C10, another brand of AS crystals of the same purity (99.5 %) was tested for comparison. Some common ions were detected in the extracts in the positive mode, but at a much lower intensity (by a factor of ~ 20, see SI9), thus demonstrating that the detected organic compounds were present in both AS crystals and that the level of organic contamination depends at least in part on the AS brand. EMSURE® products are supposed to offer a high level of quality and appear to be less contaminated despite the same reported purity. Figure 8 shows the MS-MS measurements operated on two ions detected in EXP C9 (see SI10 for the complete MS-MS results). These results support the proposed raw formula, confirming that these organic compounds contained oxygen and nitrogen and/or sulfur. They also show recurrent fragments: for instance, fragment ion at m/z 96.082, most likely described by the raw formula C<sub>6</sub>H<sub>10</sub>N, was found in all the MS-MS spectra as well as the fragment ion at m/z 69.072 corresponding to C<sub>5</sub>H<sub>9</sub> which was also a fragment observed in the spectra from the HR-ToF-AMS with high intensity.



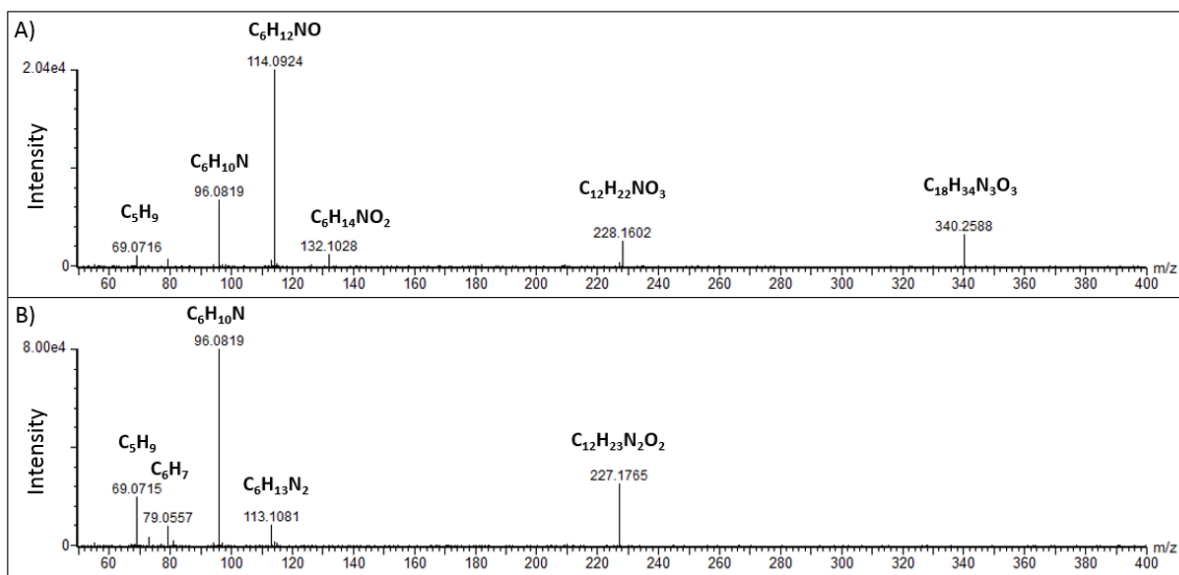


**Figure 8:** Mass spectra obtained from LC/ESI<sup>+</sup>-MS-MS measurements of two detected compounds in EXP C9. The [M+H]<sup>+</sup> ions were detected at : A) m/z 340, using a collision energy of 25 eV; and B) m/z 227, using a collision energy of 20 eV.

380

These results confirm that the organic compounds present in AS are large molecules: out of the 20 most intense detected molecules, 12 contained 12 carbon atoms (C<sub>12</sub>), and the others contained C<sub>6</sub> (2 molecules bearing C<sub>x</sub>H<sub>y</sub>N<sub>1/2</sub>), C<sub>10</sub> (1 molecule), C<sub>11</sub> (1 molecule), C<sub>17</sub> (1 molecule), C<sub>18</sub> (2 molecules) and up to C<sub>24</sub> (1 molecule), with m/z ranging from 96 to 533. Apart from the 2 smallest molecules (C<sub>6</sub>), all of them bear mono- or poly-functional groups with at least 2 heteroatoms (N and O are always present, and S is found in 10 molecules) confirming their low volatility. Most of them fragment following the same scheme, thus showing similar structures. No structure is proposed here as there are many possible structures. The fact that these molecules were largely detected in the positive mode and that they all bear at least one N atom, and the fact that they were observed specifically at the surface of the AS aerosol particles, could suggest that they are cationic surfactants such as quaternary ammonium salts remaining from the manufacturing processes. Ammonium sulfate is typically produced by the reaction of gaseous ammonia with sulfuric acid, but the precise manufacturing processes and raw materials of the suppliers are not known in detail and therefore do not allow us to draw any conclusions for these processes.

### 3.5 Removing organic traces from AS aerosol particles

To give recommendations on the use of AS for laboratory studies or instrument calibrations with organic contaminations as low as possible, the results of EXP P2 to P5 using high quality water and AS or purified AS crystals, are shown in Figure 9 where [Org]/[Sulfate] is plotted versus particle size.

395

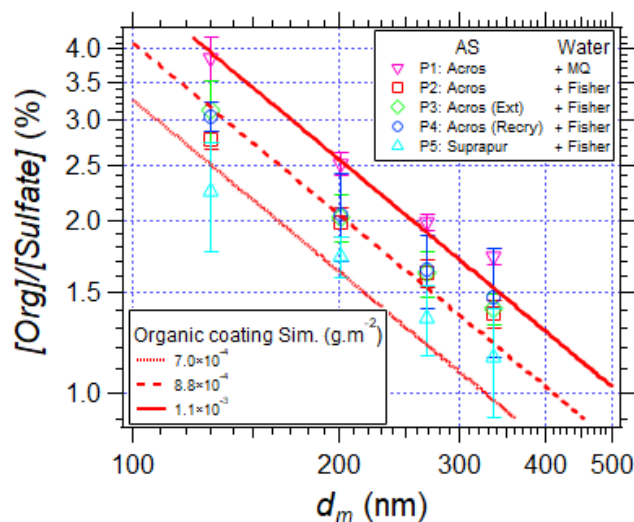


**Figure 9 :** [Org]/[Sulfate] in AS aerosol particles as function of mobility diameter in EXP P1 to P5. The red lines represent the calculated [Org]/[Sulfate] simulating surface coating of organic matter (from Eq. 3) for EXP P1, P4 and P5.

400 Figure 9 shows that, although decreasing with increasing purification, organic traces remain present in all experiments. They seem to remain coated at the surface of the particles, as shown by the good agreement between the simulations and experimental data. According to the simulation results, a reduction of 20 % of [Org]/[Sulfate] ratios is observed when Fisher water (red squares) replaces Milli-Q water (pink squares). This reduction might be due to the removing of Nylon polymers found in Milli-Q water (Fig. 7). However, no significant difference is observed between EXP P2, P3 and P4, i.e.,  
 405 purification of AS crystals by acetonitrile or recrystallization are not sufficiently efficient to remove organic traces. Finally, comparing EXP P5 (cyan squares) and P2 (red squares), another 20 % reduction of organic traces is observed when highly pure AS crystals were used (99.9999 %). In this case, the organic traces are lower than 2.5 % on the AS particles with  $d_m = 130$  to 336 nm (corresponding to  $d_a = 200$  to 500 nm).

#### 4. Conclusions and implications

410 Ammonium sulfate is one of the dominant components of atmospheric aerosol and is widely used in laboratory experiments and for instrument calibration purposes. However, the widely used commercial AS crystals may contain interfering organic impurities. To answer questions related to the quantity and the quality of organic impurities found in widely used commercial AS products, a series of experiments were performed to quantify and identify organic impurities on AS aerosol particles and in liquid solutions using a HR-ToF-AMS and a LC-MS. The results showed that, using 99.5 % purity AS,  
 415 up to 3.8 % of organic impurities were present related to sulfate mass. This ratio was found to be independent of the concentration of nebulized AS solutions but was inversely related to the particle size. The simulations of AS-Organic mixtures showed a homogeneous organic coating on the surface of AS particles with a constant surface density of  $1.1 \times 10^{-3} \text{ g.m}^{-2}$ .

Regarding the particle size selection system, the comparison between AAC and DMA showed consistent [Org]/[Sulfate] mass ratios, thus highlighting that the observed particle size effects were not due to instrumental artifacts. Using LC-MS analysis of the organic content showed up to 20 different stable highly functionalized molecules with nitrate, amin, and/or sulphate groups. The proposed raw formulas included mostly C<sub>12</sub> compounds with mono- or poly-functional groups with at least two heteroatoms (N and O were always present, and S was found in 10 molecules) suggesting low volatility. These nitrogenous molecules were abundantly detected by LC-MS in AS solutions in the positive ESI mode, and in the nebulized solutions, they were observed to be coated on the surface of AS aerosol particles. Thus, it could be suggested that they might comprise cationic surfactants such as quaternary ammonium salts remaining from the manufacturing processes.

From this suggestion, the potential effects of organic impurities on CCN activation of AS aerosols were investigated, to determine the error made on the critical supersaturation if one assumes 100% AS, omitting the presence of organic impurities. This estimation was performed with a simple calculation using the  $\kappa$ -Köhler equation (Petters and Kreidenweis, 2007), see SI11 for details. For the estimation of the critical supersaturation in the presence of organic impurities, two extreme hypotheses were explored. In hypothesis 1, the organic fraction was considered soluble and non-surface-active, whereas in hypothesis 2, it was considered extremely surface-active, using the most powerful surfactant as a proxy. Following each of these hypotheses, the supersaturation was calculated along the droplet activation of an AS particle of 130 nm with and without organic impurities (Fig. SI11). The results show that whereas the critical supersaturation of AS aerosols is not significantly impacted by the presence of organic impurities under hypothesis 1, it is highly impacted under hypothesis 2, with a potential error of more than 70%.

In view of these extreme results, and especially the very important error observed for surface-active compounds, the potential quantity of surface-active species contained in AS solutions (Across 99.5 % diluted in Milli-Q water) was investigated (SI12). The results showed that AS solutions contain extremely low amounts of cationic and non-ionic surfactants and an upper limit of [Org surfactant]/[Sulfate] mass ratio of  $1 \times 10^{-5}$  % was determined. Although this ratio is five orders of magnitude lower than the total organic fraction detected in AS particles, the potential effect of these surfactants on the surface tension of 130 nm diameter AS particles was investigated. For such particles, the obtained [Org surfactant]/[Sulfate] mass ratio induces a concentration of  $6 \times 10^{-7}$  mol.L<sup>-1</sup> of surfactants. At this very low concentration, even the most surface-active molecules show a surface tension similar to that of pure water as shown by surface tension isotherms (Ekström et al., 2010; Frossard et al., 2019; Arabadzhieva et al., 2020). It was thus concluded that the CCN activity of AS particles with  $d_m = 130$  nm should not be significantly affected by the presence of the organic impurities. However, caution should be taken to keep their amounts as low as possible.

In this work, some efforts to remove these organic impurities have been tentatively tested by purifying and recrystallizing AS crystals. Though no significant difference was observed, it is likely that better results could be obtained by increasing the number of purification and recrystallization cycles, as very high purity AS crystals (99.9999 %) showed significantly lower organic content. It is therefore recommended to use AS seeds with caution, especially when small particles are used, in terms of AS purity and water purity when aqueous solutions are used for atomization.

## Appendix A: Morphological properties of AS aerosols

Following the method of Zelenyuk et al., (2006), the shape factor ( $\chi$ ) in any flow regime (continuous and transient) can be determined by the ratio of  $d_{va}/d_m$  in Eq. A1.

$$\frac{d_{va}}{d_m} = \frac{\rho_p}{\rho_0} \frac{1}{\chi^2} \frac{C_c(d_{va}\chi\rho_p/\rho_0)}{C_c(d_m)} \quad (\text{A1})$$

455 Where  $\rho_p$  is the particle density,  $\rho_0$  is the standard density noticed as 1 g cm<sup>-3</sup>,  $C_c$  is the Cunningham slip factor (Kim et al., 2005), given by Eq. A2.

$$C_c(K_n) = 1 + K_n \left[ 1.165 + 0.483 \exp\left(-\frac{0.997}{K_n}\right) \right] \quad (\text{A2})$$

$K_n(d) = 2\lambda_g/d$  is the Knudsen number, and  $\lambda_g$  is the gas mean free path. In this work, normal temperature and pressure (293.15 K at 1 atm) were applied for the calculation of the shape factor of AS aerosols.

460 The shape factor ( $\chi$ ) of monodisperse AS aerosols selected by the AAC was calculated according to Eq. A1 and is shown in Table A1, together with the aerodynamic diameter ( $d_a$ ) selected in the AAC, the mobility diameter  $d_m$  and the vacuum aerodynamic diameter  $d_{va}$  representing the average mode of size distributions given by the SMPS and HR-ToF-AMS (p-ToF mode), respectively. Table A1 shows that, within the uncertainty, the selected AS particles own a size-independent shape factor of 1.06, which falls in the interval of 1.03 and 1.07 reported by (Zelenyuk et al., 2006).

465 Table A1: Morphological properties of monodisperse AS aerosols selected by the AAC (in EXP P1 and P2): aerodynamic diameter ( $d_a$ ), mobility diameter ( $d_m$ ), vacuum aerodynamic diameter ( $d_{va}$ ), and shape factor ( $\chi$ ). The uncertainty represents the standard deviation of several measurements under the same selection condition.

$d_a$ (nm)	$d_m$ (nm)	$d_{va}$ (nm)	Shape factor ( $\chi$ )
200	126.6 ± 0.3	206 ± 6	1.05 ± 0.02
300	194.3 ± 0.3	312 ± 8	1.06 ± 0.02
400	267.6 ± 0.4	429 ± 10	1.06 ± 0.02
500	340.3 ± 0.4	539 ± 11	1.07 ± 0.02

### Author contribution

470 JW and AM provided the initial idea of this work. JW and BTR performed the experiments and data analysis of AS aerosol characterization with the HR-ToF-AMS. NB and SR carried out the measurements of AS solutions with the LC-MS. JW, NB and JLC proposed different purification processes of AS aerosols. The organic-inorganic mixing model was provided firstly by JW and improved by BTR and AM. JW, NB, JMGS and AM developed the structure of this paper. JW summarized all contributions and expressed them in this paper. All authors provided advice regarding improvements of this paper as well as to the writing of the final version of the manuscript.

## 475 Acknowledgements

The authors acknowledge the support from the French National Research Agency (ANR-PRCI) through the projects PARAMOUNT (ANR18-CE92-0038-02) and ORACLE (ANR-20-CE93-0008-01\_ACT), as well as the French CNRS-LEFE-CHAT (Programme National-Les Enveloppes Fluides et l'Environnement-Chimie Atmosphérique – Project “SURFACTs”). The authors would like to thank two colleagues, Jim GRISILLON and Fabien ROBERT-PEILLARD, from the laboratory LCE  
480 - Aix Marseille University, who performed additional measurements for the quantification of surfactants in an AS solution. Finally, the authors acknowledge the 1<sup>st</sup> anonymous reviewer for her/his extremely thorough comments on the manuscript!

## References

- Abbatt, J. P. D., Broekhuizen, K., and Pradeep Kumar, P.: Cloud condensation nucleus activity of internally mixed ammonium sulfate/organic acid aerosol particles, *Atmos. Environ.*, 39, 4767–4778, <https://doi.org/10.1016/j.atmosenv.2005.04.029>, 2005.
- 485 Aiken, A. C., DeCarlo, P. F., and Jimenez, J. L.: Elemental Analysis of Organic Species with Electron Ionization High-Resolution Mass Spectrometry, *Anal. Chem.*, 79, 8350–8358, <https://doi.org/10.1021/ac071150w>, 2007.
- Andreae, M. O. and Rosenfeld, D.: Aerosol–cloud–precipitation interactions. Part 1. The nature and sources of cloud-active aerosols, *Earth-Sci. Rev.*, 89, 13–41, <https://doi.org/10.1016/j.earscirev.2008.03.001>, 2008.
- Arabadzhieva, D., Tchoukov, P., and Mileva, E.: Impact of Adsorption Layer Properties on Drainage Behavior of Microscopic  
490 Foam Films: The Case of Cationic/Nonionic Surfactant Mixtures, *Colloids Interfaces*, 4, 53, <https://doi.org/10.3390/colloids4040053>, 2020.
- Badger, C. L., George, I., Griffiths, P. T., Braban, C. F., Cox, R. A., and Abbatt, J. P. D.: Phase transitions and hygroscopic growth of aerosol particles containing humic acid and mixtures of humic acid and ammonium sulphate, *Atmospheric Chem. Phys.*, 6, 755–768, <https://doi.org/10.5194/acp-6-755-2006>, 2006.
- 495 Brooks, S. D., DeMott, P. J., and Kreidenweis, S. M.: Water uptake by particles containing humic materials and mixtures of humic materials with ammonium sulfate, *Atmos. Environ.*, 38, 1859–1868, <https://doi.org/10.1016/j.atmosenv.2004.01.009>, 2004.
- Brüggemann, M., Xu, R., Tilgner, A., Kwong, K. C., Mutzel, A., Poon, H. Y., Otto, T., Schaefer, T., Poulain, L., Chan, M. N., and Herrmann, H.: Organosulfates in Ambient Aerosol: State of Knowledge and Future Research Directions on Formation,  
500 Abundance, Fate, and Importance, *Environ. Sci. Technol.*, 54, 3767–3782, <https://doi.org/10.1021/acs.est.9b06751>, 2020.
- Canagaratna, M. R., Jimenez, J. L., Kroll, J. H., Chen, Q., Kessler, S. H., Massoli, P., Hildebrandt Ruiz, L., Fortner, E., Williams, L. R., Wilson, K. R., Surratt, J. D., Donahue, N. M., Jayne, J. T., and Worsnop, D. R.: Elemental ratio measurements of organic compounds using aerosol mass spectrometry: characterization, improved calibration, and implications, *Atmospheric Chem. Phys.*, 15, 253–272, <https://doi.org/10.5194/acp-15-253-2015>, 2015.
- 505 Charlson, R. J., Schwartz, S., Hales, J., Cess, R. D., Coakley, J. J., Hansen, J., and Hofmann, D.: Climate forcing by anthropogenic aerosols, *Science*, 255, 423–430, 1992.

- Clegg, S. L., Brimblecombe, P., and Wexler, A. S.: Thermodynamic Model of the System  $\text{H}^+ - \text{NH}_4^+ - \text{Na}^+ - \text{SO}_4^{2-} - \text{NO}_3^- - \text{Cl}^- - \text{H}_2\text{O}$  at 298.15 K, *J. Phys. Chem. A*, 102, 2155–2171, <https://doi.org/10.1021/jp973043j>, 1998.
- 510 Darer, A. I., Cole-Filipiak, N. C., O'Connor, A. E., and Elrod, M. J.: Formation and stability of atmospherically relevant isoprene-derived organosulfates and organonitrates, *Environ. Sci. Technol.*, 45, 1895–1902, 2011.
- De Haan, D. O., Hawkins, L. N., Welsh, H. G., Pednekar, R., Casar, J. R., Pennington, E. A., de Loera, A., Jimenez, N. G., Symons, M. A., Zauscher, M., Pajunoja, A., Caponi, L., Cazaunau, M., Formenti, P., Gratien, A., Pangui, E., and Doussin, J.-F.: Brown Carbon Production in Ammonium- or Amine-Containing Aerosol Particles by Reactive Uptake of Methylglyoxal and Photolytic Cloud Cycling, *Environ. Sci. Technol.*, 51, 7458–7466, <https://doi.org/10.1021/acs.est.7b00159>, 2017.
- 515 DeCarlo, P. F., Slowik, J. G., Worsnop, D. R., Davidovits, P., and Jimenez, J. L.: Particle Morphology and Density Characterization by Combined Mobility and Aerodynamic Diameter Measurements. Part 1: Theory, *Aerosol Sci. Technol.*, 38, 1185–1205, <https://doi.org/10.1080/027868290903907>, 2004.
- DeCarlo, P. F., Kimmel, J. R., Trimborn, A., Northway, M. J., Jayne, J. T., Aiken, A. C., Gonin, M., Fuhrer, K., Horvath, T., Docherty, K. S., Worsnop, D. R., and Jimenez, J. L.: Field-Deployable, High-Resolution, Time-of-Flight Aerosol Mass  
520 Spectrometer, *Anal. Chem.*, 78, 8281–8289, <https://doi.org/10.1021/ac061249n>, 2006.
- Ekström, S., Nozière, B., Hultberg, M., Alsberg, T., Magnér, J., Nilsson, E. D., and Artaxo, P.: A possible role of ground-based microorganisms on cloud formation in the atmosphere, *Biogeosciences*, 7, 387–394, <https://doi.org/10.5194/bg-7-387-2010>, 2010.
- Engelhart, G. J., Asa-Awuku, A., Nenes, A., and Pandis, S. N.: CCN activity and droplet growth kinetics of fresh and aged  
525 monoterpene secondary organic aerosol, *Atmospheric Chem. Phys.*, 8, 3937–3949, <https://doi.org/10.5194/acp-8-3937-2008>, 2008.
- Frossard, A. A., Gérard, V., Duplessis, P., Kinsey, J. D., Lu, X., Zhu, Y., Bisgrove, J., Maben, J. R., Long, M. S., Chang, R. Y.-W., Beaupré, S. R., Kieber, D. J., Keene, W. C., Nozière, B., and Cohen, R. C.: Properties of Seawater Surfactants Associated with Primary Marine Aerosol Particles Produced by Bursting Bubbles at a Model Air–Sea Interface, *Environ. Sci.*  
530 *Technol.*, 53, 9407–9417, <https://doi.org/10.1021/acs.est.9b02637>, 2019.
- Gérard, V., Nozière, B., Fine, L., Ferronato, C., Singh, D. K., Frossard, A. A., Cohen, R. C., Asmi, E., Lihavainen, H., Kivekäs, N., Aurela, M., Brus, D., Frka, S., and Cvitešić Kušan, A.: Concentrations and Adsorption Isotherms for Amphiphilic Surfactants in PM1 Aerosols from Different Regions of Europe, *Environ. Sci. Technol.*, 53, 12379–12388, <https://doi.org/10.1021/acs.est.9b03386>, 2019.
- 535 Grace, D. N., Lugos, E. N., Ma, S., Griffith, D. R., Hendrickson, H. P., Woo, J. L., and Galloway, M. M.: Brown Carbon Formation Potential of the Biacetyl–Ammonium Sulfate Reaction System, *ACS Earth Space Chem.*, 4, 1104–1113, <https://doi.org/10.1021/acsearthspacechem.0c00096>, 2020.
- Hämeri, K., Charlson, R., and Hansson, H.-C.: Hygroscopic properties of mixed ammonium sulfate and carboxylic acids particles, *AIChE J.*, 48, 1309–1316, <https://doi.org/10.1002/aic.690480617>, 2002.

- 540 Hawkins, L. N., Welsh, H. G., and Alexander, M. V.: Evidence for pyrazine-based chromophores in cloud water mimics containing methylglyoxal and ammonium sulfate, *Atmospheric Chem. Phys.*, 18, 12413–12431, <https://doi.org/10.5194/acp-18-12413-2018>, 2018.
- Hensley, J. C., Birdsall, A. W., Valtierra, G., Cox, J. L., and Keutsch, F. N.: Revisiting the reaction of dicarbonyls in aerosol proxy solutions containing ammonia: the case of butenedial, *Atmospheric Chem. Phys.*, 21, 8809–8821, <https://doi.org/10.5194/acp-21-8809-2021>, 2021.
- 545 Herrmann, H.: Kinetics of Aqueous Phase Reactions Relevant for Atmospheric Chemistry, *Chem. Rev.*, 103, 4691–4716, <https://doi.org/10.1021/cr020658q>, 2003.
- Hu, K. S., Darer, A. I., and Elrod, M. J.: Thermodynamics and kinetics of the hydrolysis of atmospherically relevant organonitrates and organosulfates, *Atmospheric Chem. Phys.*, 11, 8307–8320, <https://doi.org/10.5194/acp-11-8307-2011>, 2011.
- 550 Iinuma, Y., Müller, C., Berndt, T., Böge, O., Claeys, M., and Herrmann, H.: Evidence for the Existence of Organosulfates from  $\beta$ -Pinene Ozonolysis in Ambient Secondary Organic Aerosol, *Environ. Sci. Technol.*, 41, 6678–6683, <https://doi.org/10.1021/es070938t>, 2007.
- IPCC: Climate Change 2013 – The Physical Science Basis: Working Group I Contribution to the Fifth Assessment Report of the Intergovernmental Panel on Climate Change, Cambridge University Press, Cambridge, <https://doi.org/10.1017/CBO9781107415324>, 2013.
- 555 Jimenez, J. L., Canagaratna, M. R., Donahue, N. M., Prevot, A. S. H., Zhang, Q., Kroll, J. H., DeCarlo, P. F., Allan, J. D., Coe, H., Ng, N. L., Aiken, A. C., Docherty, K. S., Ulbrich, I. M., Grieshop, A. P., Robinson, A. L., Duplissy, J., Smith, J. D., Wilson, K. R., Lanz, V. A., Hueglin, C., Sun, Y. L., Tian, J., Laaksonen, A., Raatikainen, T., Rautiainen, J., Vaattovaara, P., Ehn, M., Kulmala, M., Tomlinson, J. M., Collins, D. R., Cubison, M. J., E, Dunlea, J., Huffman, J. A., Onasch, T. B., Alfarra, M. R., Williams, P. I., Bower, K., Kondo, Y., Schneider, J., Drewnick, F., Borrmann, S., Weimer, S., Demerjian, K., Salcedo, D., Cottrell, L., Griffin, R., Takami, A., Miyoshi, T., Hatakeyama, S., Shimo, A., Sun, J. Y., Zhang, Y. M., Dzepina, K., Kimmel, J. R., Sueper, D., Jayne, J. T., Herndon, S. C., Trimborn, A. M., Williams, L. R., Wood, E. C., Middlebrook, A. M., Kolb, C. E., Baltensperger, U., and Worsnop, D. R.: Evolution of Organic Aerosols in the Atmosphere, *Science*, 326, 1525–1529, <https://doi.org/10.1126/science.1180353>, 2009.
- 565 Jimenez, N. G., Sharp, K. D., Gramyk, T., Uglund, D. Z., Tran, M.-K., Rojas, A., Rafla, M. A., Stewart, D., Galloway, M. M., Lin, P., Laskin, A., Cazaunau, M., Pangu, E., Doussin, J.-F., and De Haan, D. O.: Radical-Initiated Brown Carbon Formation in Sunlit Carbonyl–Amine–Ammonium Sulfate Mixtures and Aqueous Aerosol Particles, *ACS Earth Space Chem.*, 6, 228–238, <https://doi.org/10.1021/acsearthspacechem.1c00395>, 2022.
- 570 Johnson, T. J., Irwin, M., Symonds, J. P. R., Olfert, J. S., and Boies, A. M.: Measuring aerosol size distributions with the aerodynamic aerosol classifier, *Aerosol Sci. Technol.*, 52, 655–665, <https://doi.org/10.1080/02786826.2018.1440063>, 2018.

- Kampf, C. J., Jakob, R., and Hoffmann, T.: Identification and characterization of aging products in the glyoxal/ammonium sulfate system &ndash; implications for light-absorbing material in atmospheric aerosols, *Atmospheric Chem. Phys.*, 12, 6323–6333, <https://doi.org/10.5194/acp-12-6323-2012>, 2012.
- 575 Keller, B. O., Sui, J., Young, A. B., and Whittall, R. M.: Interferences and contaminants encountered in modern mass spectrometry, *Anal. Chim. Acta*, 627, 71–81, <https://doi.org/10.1016/j.aca.2008.04.043>, 2008.
- Kiendler-Scharr, A., Mensah, A. A., Friese, E., Topping, D., Nemitz, E., Prevot, A. S. H., Äijälä, M., Allan, J., Canonaco, F., Canagaratna, M., Carbone, S., Crippa, M., Dall'Osto, M., Day, D. A., De Carlo, P., Di Marco, C. F., Elbern, H., Eriksson, A., Freney, E., Hao, L., Herrmann, H., Hildebrandt, L., Hillamo, R., Jimenez, J. L., Laaksonen, A., McFiggans, G., Mohr, C.,
- 580 O'Dowd, C., Otjes, R., Ovadnevaite, J., Pandis, S. N., Poulain, L., Schlag, P., Sellegri, K., Swietlicki, E., Tiitta, P., Vermeulen, A., Wahner, A., Worsnop, D., and Wu, H.-C.: Ubiquity of organic nitrates from nighttime chemistry in the European submicron aerosol, *Geophys. Res. Lett.*, 43, 7735–7744, <https://doi.org/10.1002/2016GL069239>, 2016.
- Kim, J. H., Mulholland, G. W., Kukuck, S. R., and Pui, D. Y. H.: Slip Correction Measurements of Certified PSL Nanoparticles Using a Nanometer Differential Mobility Analyzer (Nano-DMA) for Knudsen Number From 0.5 to 83, *J. Res. Natl. Inst. Stand. Technol.*, 110, 31–54, <https://doi.org/10.6028/jres.110.005>, 2005.
- 585 Kind, T. and Fiehn, O.: Seven Golden Rules for heuristic filtering of molecular formulas obtained by accurate mass spectrometry, *BMC Bioinformatics*, 8, 105, <https://doi.org/10.1186/1471-2105-8-105>, 2007.
- King, S. M., Rosenoern, T., Shilling, J. E., Chen, Q., and Martin, S. T.: Increased cloud activation potential of secondary organic aerosol for atmospheric mass loadings, *Atmospheric Chem. Phys.*, 9, 2959–2971, [https://doi.org/10.5194/acp-9-2959-](https://doi.org/10.5194/acp-9-2959-2009)
- 590 2009, 2009.
- Koehler, K. A., Kreidenweis, S. M., DeMott, P. J., Prenni, A. J., Carrico, C. M., Ervens, B., and Feingold, G.: Water activity and activation diameters from hygroscopicity data - Part II: Application to organic species, *Atmospheric Chem. Phys.*, 6, 795–809, <https://doi.org/10.5194/acp-6-795-2006>, 2006.
- Laskin, J., Laskin, A., Nizkorodov, S. A., Roach, P., Eckert, P., Gilles, M. K., Wang, B., Lee, H. J. (Julie), and Hu, Q.:
- 595 Molecular Selectivity of Brown Carbon Chromophores, *Environ. Sci. Technol.*, 48, 12047–12055, <https://doi.org/10.1021/es503432r>, 2014.
- Meyer, N. K., Duplissy, J., Gysel, M., Metzger, A., Dommen, J., Weingartner, E., Alfarra, M. R., Prevot, A. S. H., Fletcher, C., Good, N., McFiggans, G., Jonsson, Å. M., Hallquist, M., Baltensperger, U., and Ristovski, Z. D.: Analysis of the hygroscopic and volatile properties of ammonium sulphate seeded and unseeded SOA particles, *Atmospheric Chem. Phys.*, 9,
- 600 721–732, <https://doi.org/10.5194/acp-9-721-2009>, 2009.
- Moore, R. H., Ingall, E. D., Sorooshian, A., and Nenes, A.: Molar mass, surface tension, and droplet growth kinetics of marine organics from measurements of CCN activity, *Geophys. Res. Lett.*, 35, <https://doi.org/10.1029/2008GL033350>, 2008.
- Nandy, L. and Dutcher, C. S.: Phase Behavior of Ammonium Sulfate with Organic Acid Solutions in Aqueous Aerosol Mimics Using Microfluidic Traps, *J. Phys. Chem. B*, 122, 3480–3490, <https://doi.org/10.1021/acs.jpcc.7b10655>, 2018.



- 605 Nozière, B., Dziedzic, P., and Córdoba, A.: Inorganic ammonium salts and carbonate salts are efficient catalysts for aldol condensation in atmospheric aerosols, *Phys. Chem. Chem. Phys.*, 12, 3864–3872, <https://doi.org/10.1039/B924443C>, 2010.
- Nozière, B., Baduel, C., and Jaffrezo, J.-L.: The dynamic surface tension of atmospheric aerosol surfactants reveals new aspects of cloud activation, *Nat. Commun.*, 5, 3335, <https://doi.org/10.1038/ncomms4335>, 2014.
- Ovadnevaite, J., Zuend, A., Laaksonen, A., Sanchez, K. J., Roberts, G., Ceburnis, D., Decesari, S., Rinaldi, M., Hodas, N.,  
610 Facchini, M. C., Seinfeld, J. H., and O’ Dowd, C.: Surface tension prevails over solute effect in organic-influenced cloud droplet activation, *Nature*, 546, 637–641, <https://doi.org/10.1038/nature22806>, 2017.
- Petters, M. D.: A language to simplify computation of differential mobility analyzer response functions, *Aerosol Sci. Technol.*, 52, 1437–1451, <https://doi.org/10.1080/02786826.2018.1530724>, 2018.
- Petters, M. D. and Kreidenweis, S. M.: A single parameter representation of hygroscopic growth and cloud condensation  
615 nucleus activity, *Atmospheric Chem. Phys.*, 7, 1961–1971, <https://doi.org/10.5194/acp-7-1961-2007>, 2007.
- Petters, M. D. and Kreidenweis, S. M.: A single parameter representation of hygroscopic growth and cloud condensation nucleus activity &ndash; Part 3: Including surfactant partitioning, *Atmospheric Chem. Phys.*, 13, 1081–1091, <https://doi.org/10.5194/acp-13-1081-2013>, 2013.
- Pieber, S. M., El Haddad, I., Slowik, J. G., Canagaratna, M. R., Jayne, J. T., Platt, S. M., Bozzetti, C., Daellenbach, K. R.,  
620 Fröhlich, R., Vlachou, A., Klein, F., Dommen, J., Miljevic, B., Jiménez, J. L., Worsnop, D. R., Baltensperger, U., and Prévôt, A. S. H.: Inorganic Salt Interference on CO<sub>2</sub><sup>+</sup> in Aerodyne AMS and ACSM Organic Aerosol Composition Studies, *Environ. Sci. Technol.*, 50, 10494–10503, <https://doi.org/10.1021/acs.est.6b01035>, 2016.
- Pöschl, U. and Shiraiwa, M.: Multiphase Chemistry at the Atmosphere–Biosphere Interface Influencing Climate and Public Health in the Anthropocene, *Chem. Rev.*, 115, 4440–4475, <https://doi.org/10.1021/cr500487s>, 2015.
- 625 Powelson, M. H., Espelien, B. M., Hawkins, L. N., Galloway, M. M., and De Haan, D. O.: Brown Carbon Formation by Aqueous-Phase Carbonyl Compound Reactions with Amines and Ammonium Sulfate, *Environ. Sci. Technol.*, 48, 985–993, <https://doi.org/10.1021/es4038325>, 2014.
- Prenni, A. J., DeMott, P. J., and Kreidenweis, S. M.: Water uptake of internally mixed particles containing ammonium sulfate and dicarboxylic acids, *Atmos. Environ.*, 37, 4243–4251, [https://doi.org/10.1016/S1352-2310\(03\)00559-4](https://doi.org/10.1016/S1352-2310(03)00559-4), 2003.
- 630 Prisle, N. L.: A predictive thermodynamic framework of cloud droplet activation for chemically unresolved aerosol mixtures, including surface tension, non-ideality, and bulk–surface partitioning, *Atmospheric Chem. Phys.*, 21, 16387–16411, <https://doi.org/10.5194/acp-21-16387-2021>, 2021.
- Saukko, E., Zorn, S., Kuwata, M., Keskinen, J., and Virtanen, A.: Phase State and Deliquescence Hysteresis of Ammonium-Sulfate-Seeded Secondary Organic Aerosol, *Aerosol Sci. Technol.*, 49, 531–537,  
635 <https://doi.org/10.1080/02786826.2015.1050085>, 2015.
- Seinfeld, J. H., Bretherton, C., Carslaw, K. S., Coe, H., DeMott, P. J., Dunlea, E. J., Feingold, G., Ghan, S., Guenther, A. B., Kahn, R., Kraucunas, I., Kreidenweis, S. M., Molina, M. J., Nenes, A., Penner, J. E., Prather, K. A., Ramanathan, V., Ramaswamy, V., Rasch, P. J., Ravishankara, A. R., Rosenfeld, D., Stephens, G., and Wood, R.: Improving our fundamental

- understanding of the role of aerosol–cloud interactions in the climate system, *Proc. Natl. Acad. Sci.*, 113, 5781–5790, <https://doi.org/10.1073/pnas.1514043113>, 2016.
- 640 Shakya, K. M. and Peltier, R. E.: Non-sulfate sulfur in fine aerosols across the United States: Insight for organosulfate prevalence, *Atmos. Environ.*, 100, 159–166, <https://doi.org/10.1016/j.atmosenv.2014.10.058>, 2015.
- Sjogren, S., Gysel, M., Weingartner, E., Baltensperger, U., Cubison, M. J., Coe, H., Zardini, A. A., Marcolli, C., Krieger, U. K., and Peter, T.: Hygroscopic growth and water uptake kinetics of two-phase aerosol particles consisting of ammonium sulfate, adipic and humic acid mixtures, *J. Aerosol Sci.*, 38, 157–171, <https://doi.org/10.1016/j.jaerosci.2006.11.005>, 2007.
- 645 Smith, M. L., You, Y., Kuwata, M., Bertram, A. K., and Martin, S. T.: Phase Transitions and Phase Miscibility of Mixed Particles of Ammonium Sulfate, Toluene-Derived Secondary Organic Material, and Water, *J. Phys. Chem. A*, 117, 8895–8906, <https://doi.org/10.1021/jp405095e>, 2013.
- Sorjamaa, R., Svenningsson, B., Raatikainen, T., Henning, S., Bilde, M., and Laaksonen, A.: The role of surfactants in Köhler theory reconsidered, *Atmospheric Chem. Phys.*, 4, 2107–2117, <https://doi.org/10.5194/acp-4-2107-2004>, 2004.
- 650 Stokes, R. H. and Robinson, R. A.: Interactions in Aqueous Nonelectrolyte Solutions. I. Solute-Solvent Equilibria, *J. Phys. Chem.*, 70, 2126–2131, <https://doi.org/10.1021/j100879a010>, 1966.
- Surratt, J. D., Gómez-González, Y., Chan, A. W. H., Vermeylen, R., Shahgholi, M., Kleindienst, T. E., Edney, E. O., Offenberg, J. H., Lewandowski, M., Jaoui, M., Maenhaut, W., Claeys, M., Flagan, R. C., and Seinfeld, J. H.: Organosulfate Formation in Biogenic Secondary Organic Aerosol, *J. Phys. Chem. A*, 112, 8345–8378, <https://doi.org/10.1021/jp802310p>, 2008.
- 655 Szmigielski, R.: Evidence for C5 organosulfur secondary organic aerosol components from in-cloud processing of isoprene: Role of reactive SO<sub>4</sub> and SO<sub>3</sub> radicals, *Atmos. Environ.*, 130, 14–22, <https://doi.org/10.1016/j.atmosenv.2015.10.072>, 2016.
- Tavakoli, F. and Olfert, J. S.: An Instrument for the Classification of Aerosols by Particle Relaxation Time: Theoretical Models of the Aerodynamic Aerosol Classifier, *Aerosol Sci. Technol.*, 47, 916–926, <https://doi.org/10.1080/02786826.2013.802761>, 2013.
- 660 Tervahattu, H., Hartonen, K., Kerminen, V.-M., Kupiainen, K., Aarnio, P., Koskentalo, T., Tuck, A. F., and Vaida, V.: New evidence of an organic layer on marine aerosols, *J. Geophys. Res. Atmospheres*, 107, AAC 1-1-AAC 1-8, <https://doi.org/10.1029/2000JD000282>, 2002.
- Trainic, M., Abo Riziq, A., Lavi, A., Flores, J. M., and Rudich, Y.: The optical, physical and chemical properties of the products of glyoxal uptake on ammonium sulfate seed aerosols, *Atmospheric Chem. Phys.*, 11, 9697–9707, <https://doi.org/10.5194/acp-11-9697-2011>, 2011.
- 665 Tran, J. C. and Doucette, A. A.: Cyclic polyamide oligomers extracted from nylon 66 membrane filter disks as a source of contamination in liquid chromatography/mass spectrometry, *J. Am. Soc. Mass Spectrom.*, 17, 652–656, <https://doi.org/10.1016/j.jasms.2006.01.008>, 2006.
- 670 Treuel, L., Pederzani, S., and Zellner, R.: Deliquescence behaviour and crystallisation of ternary ammonium sulfate/dicarboxylic acid/water aerosols, *Phys. Chem. Chem. Phys.*, 11, 7976–7984, <https://doi.org/10.1039/B905007H>, 2009.

- Varutbangkul, V., Brechtel, F. J., Bahreini, R., Ng, N. L., Keywood, M. D., Kroll, J. H., Flagan, R. C., Seinfeld, J. H., Lee, A., and Goldstein, A. H.: Hygroscopicity of secondary organic aerosols formed by oxidation of cycloalkenes, monoterpenes, sesquiterpenes, and related compounds, *Atmospheric Chem. Phys.*, 6, 2367–2388, <https://doi.org/10.5194/acp-6-2367-2006>, 2006.
- 675 Vepsäläinen, S., Calderón, S. M., Malila, J., and Prisle, N. L.: Comparison of six approaches to predicting droplet activation of surface active aerosol – Part 1: moderately surface active organics, *Atmospheric Chem. Phys.*, 22, 2669–2687, <https://doi.org/10.5194/acp-22-2669-2022>, 2022.
- 680 Wach, P., Spólnik, G., Rudziński, K. J., Skotak, K., Claeys, M., Danikiewicz, W., and Szmigielski, R.: Radical oxidation of methyl vinyl ketone and methacrolein in aqueous droplets: Characterization of organosulfates and atmospheric implications, *Chemosphere*, 214, 1–9, <https://doi.org/10.1016/j.chemosphere.2018.09.026>, 2019.
- Wex, H., Petters, M. D., Carrico, C. M., Hallbauer, E., Massling, A., McMeeking, G. R., Poulain, L., Wu, Z., Kreidenweis, S. M., and Stratmann, F.: Towards closing the gap between hygroscopic growth and activation for secondary organic aerosol: Part 1 – Evidence from measurements, *Atmospheric Chem. Phys.*, 9, 3987–3997, <https://doi.org/10.5194/acp-9-3987-2009>, 2009.
- 685 Wiedensohler, A., Birmili, W., Nowak, A., Sonntag, A., Weinhold, K., Merkel, M., Wehner, B., Tuch, T., Pfeifer, S., Fiebig, M., Fjåraa, A. M., Asmi, E., Sellegri, K., Depuy, R., Venzac, H., Villani, P., Laj, P., Aalto, P., Ogren, J. A., Swietlicki, E., Williams, P., Roldin, P., Quincey, P., Hüglin, C., Fierz-Schmidhauser, R., Gysel, M., Weingartner, E., Riccobono, F., Santos, S., Gröning, C., Faloon, K., Beddows, D., Harrison, R., Monahan, C., Jennings, S. G., O’Dowd, C. D., Marinoni, A., Horn, H.-G., Keck, L., Jiang, J., Scheckman, J., McMurry, P. H., Deng, Z., Zhao, C. S., Moerman, M., Henzing, B., de Leeuw, G., Lösschau, G., and Bastian, S.: Mobility particle size spectrometers: harmonization of technical standards and data structure to facilitate high quality long-term observations of atmospheric particle number size distributions, *Atmospheric Meas. Tech.*, 5, 657–685, <https://doi.org/10.5194/amt-5-657-2012>, 2012.
- 690 Zelenyuk, A., Cai, Y., and Imre, D.: From Agglomerates of Spheres to Irregularly Shaped Particles: Determination of Dynamic Shape Factors from Measurements of Mobility and Vacuum Aerodynamic Diameters, *Aerosol Sci. Technol.*, 40, 197–217, <https://doi.org/10.1080/02786820500529406>, 2006.